Self-Assembly of Linear Arrays of Semiconductor Nanoparticles on Carbon Single-Walled Nanotubes†

Chaiwat Engtrakul,* Yong-Hyun Kim, Jovan M. Nedeljković, S. Phil Ahrenkiel, Katherine E. H. Gilbert, Jeff L. Alleman, S. B. Zhang, Olga I. Mićić, Arthur J. Nozik, and Michael J. Heben*

National Renewable Energy Laboratory, 1617 Cole Boulevard, Golden, Colorado 80401

Received: August 10, 2006

Ligand-stabilized nanocrystals (NCs) were strongly bound to the nanotube surfaces by simple van der Waals forces. Linear arrays of CdSe and InP quantum dots were formed by self-assembly using the grooves in bundles of carbon single-walled nanotubes (SWNTs) as a one-dimensional template. A simple geometrical model explains the ordering in terms of the anisotropic properties of the nanotube surface. CdSe quantum rods were also observed to self-organize onto SWNTs with their long axis parallel to the nanotube axis. This approach offers a route to the formation of ordered NC/SWNT architectures that avoids problems associated with surface derivatization.

Both semiconductor quantum dots (QDs)[1] and carbon single-walled nanotubes (SWNTs)[2] possess interesting and potentially useful optical and electronic properties due to their nanoscale structures. In the case of QDs, quantum confinement in three dimensions produces a size-dependent modification of the electronic band structure, resulting in the formation of discrete electronic states. QDs exhibit unique behaviors such as efficient photoluminescence and photon up-conversion, slowed relaxation and cooling of hot carriers, enhanced lasing, and carrier multiplication via impact ionization.[3] SWNTs, however, consist of sp^2-hybridized carbon atoms that form the walls of nanometer-wide, seamless cylinders.[4] The SWNT electronic structure is controlled by the nanotube's circumferential periodicity.[5] The tube structure gives rise to highly anisotropic optical properties, strongly coupled electronic and vibrational states, ballistic carrier transport, and efficient field emission.[6−8] The unique electronic properties of QDs and SWNTs suggest that architectures constructed from combinations of these nanoscale building blocks would also exhibit interesting and useful properties.[9,10] For example, one can envision sensitive and selective sensors, low-power, fast transistors, as well as new approaches to managing charge, energy, and mass transfer on the nanoscale for improved solar energy conversion and photocatalysis.[11] To explore these possibilities, however, general methods must be developed for the construction of well-defined QD/SWNT heterostructures.

Past efforts to attach semiconductor nanocrystals (NCs) to nanotubes have focused on forming chemical attachments between the two different nanostructures. In this approach, defects in the nanotube lattice, i.e., any site where the sp^2-bonded carbon network is broken, are used as sites for chemical bond formation. Such defects are typically present after acid-based purification methods or may be specifically introduced by chemical derivatization.[12−18] For example, Haremza et al.[12] coupled amine-functionalized CdSe quantum dots to acid-chloride-modified SWNTs via amide bond formation. Li et al.[16] labeled the defects on oxidized SWNTs using TiO_2 nanoparticles as markers, and Banerjee et al.[17,18] studied the in situ growth of cadmium telluride NCs at oxygen-terminated sites on acid-oxidized carbon nanotube surfaces. Nanoparticles are attached in each of these cases via a chemical linkage at the point where the sp^2-bonded nanotube lattice is disrupted. As a result, the electronic structure of the carbon nanotube is likely to be compromised at the attachment site. In extreme cases, an attempt to attach many QDs would result in the destruction of the tube. The chemical attachment strategy is also difficult to control since the location of the defective carbon atom or the site for derivatization cannot be specified at this time. Covalent attachment methods currently lead to random and poorly organized nanoparticle coatings. Alternatively, Guldi et al.[19] linked CdTe NCs to carbon nanotubes through electrostatic interactions producing photoactive nanohybrid structures and concluded that noncovalent methods for integrating semiconductor NCs with carbon nanotubes appeared particularly promising.

In this paper, we report the formation of organized, one-dimensional (1-D) arrays of semiconductor QDs by van der Waals (vdW) adsorption onto SWNTs. Two representative II−VI and the III−V semiconductor NCs, CdSe and InP, respectively, demonstrated linear ordering when adsorbed from nonaqueous colloidal solutions onto high-purity, low-defect-density SWNTs. The tendency to form linear arrays was greatest when tube−tube alignment was relatively good within bundles and when the QDs were relatively large. The edge-to-edge (e−e) separation distance between QDs in the 1-D arrays was ∼18 Å for both the InP and the CdSe QDs, indicating that QD−QD separation is governed by the thickness of the ligand shells, as is the case in two- and three-dimensional QD arrays.[20−23] Surface derivatization and covalent linkages were not required for binding. Consequently, the optical absorption properties of the SWNTs were not degraded by the formation of the composites. The linear self-assembly is explained by considering the vdW forces between QDs and the grooves in SWNT bundles. The vdW forces also cause quantum rods (QRs) to adsorb onto SWNT surfaces with the QR's long axis aligned parallel to the nanotube axes and some tendency for head-to-

† Part of the special issue "Arthur J. Nozik Festschrift".

* Authors to whom correspondence should be addressed. E-mail: chaiwat_engtrakul@nrel.gov; michael_heben@nrel.gov.

10.1021/jp065176n CCC: $33.50
Published on Web 10/20/2006

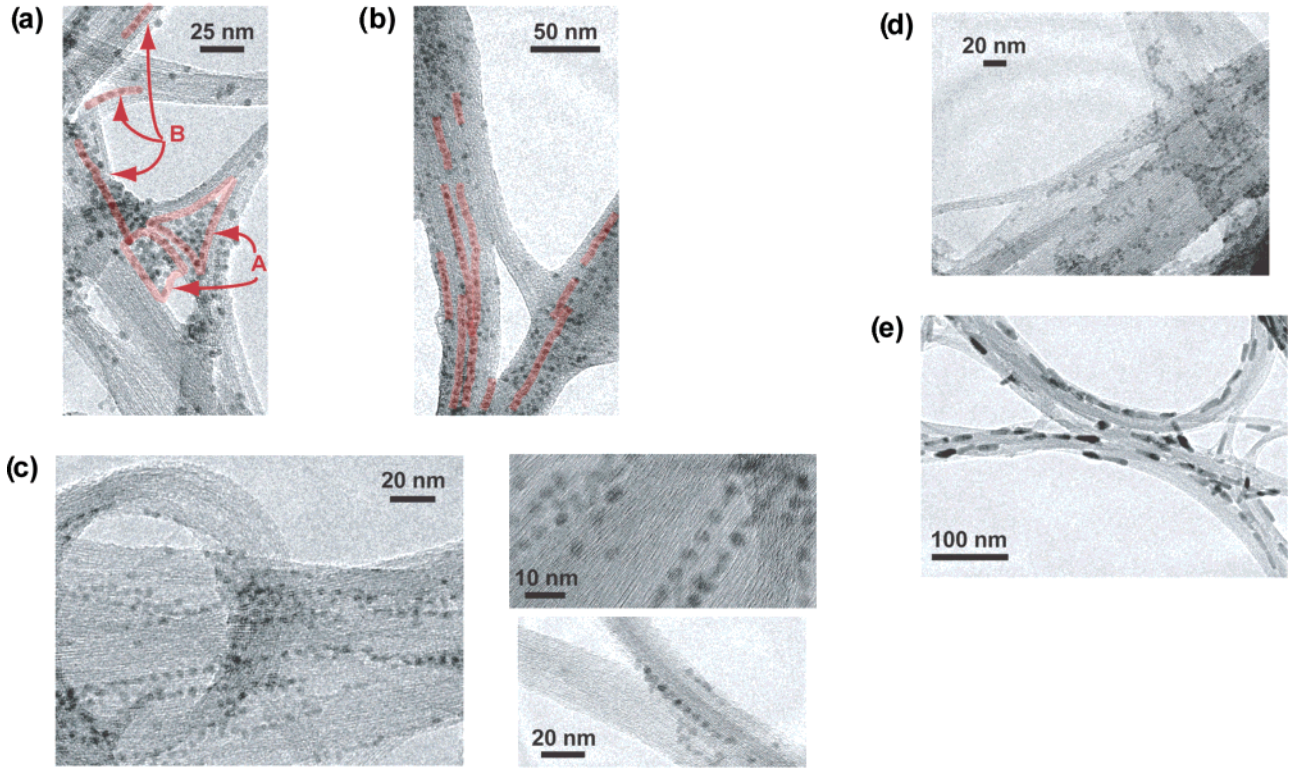

Figure 1. TEM images of InP QDs (sample 1) (a) packed between intersecting SWNT bundles (labeled A) as well as short, linear arrays of InP QDs adsorbed to the SWNTs parallel to the nanotube axes (labeled B) and (b) clearly showing the tendency for the QDs to align in chains extending along the axes of the SWNT bundles. Highlighting in red serves as a guide to the eye. (c) TEM image of CdSe QDs (sample 2) adsorbed to the SWNT surfaces in linear chains as long as 20 QDs. High-resolution TEM images of these assemblies show a c−c separation distance of 53 ± 1 Å, indicating a QD−QD edge separation of ∼18 Å. TEM micrographs of (d) CdSe QD/SWNT assemblies (sample 3) showing little organization, while (e) linear chains as long as six CdSe QRs (sample 4) were observed on the surfaces of the SWNT bundles.

toe alignment. In general, the findings described here indicate a new and potentially powerful route to the formation of useful NC/SWNT architectures differing from traditional methodologies for assembling 1-D arrays of NCs from zero-dimensional NCs.[24,25] Our method for integrating the two materials does not impart any functionalization to the nanotube surface, and therefore, the integrity and electronic structure of the SWNT are maintained by not incorporating sp^3 sites into the carbon nanotube lattice.

SWNT materials were synthesized by laser vaporization and purified in a two-step purification process.[26] The purified nanotube paper was determined to be ∼95 wt % pure by a combination of Raman spectroscopy, thermal gravimetric analysis, and transmission electron microscopy (TEM). Raman spectroscopy showed a very low ratio between the D-band and G-band modes (∼1/190) at 488 nm, indicating a low number of defects and sp^3-bonded carbon species.[27] Trioctylphosphine/trioctylphosphine oxide (TOP/TOPO) stabilized InP and CdSe QDs, and CdSe QRs were synthesized and purified according to previously reported methods.[28−31] The size distribution of the InP QDs was reduced by size-selective precipitation. The NC diameters were determined by optical absorption spectroscopy and TEM. TEM specimens were prepared by depositing 1 μL of solution onto a lacey carbon grid (Ted Pella) and drying in a vacuum for 1 h. TEM was performed with a Philips CM30 instrument at 200 kV. Energy-dispersive X-ray analysis confirmed the chemical composition of the QDs and QRs to be that of the starting materials.

The purified SWNT materials were dispersed in toluene (3 mg/3 mL) by sonication for 5 min and stirred for 18 h at 80 °C under nitrogen. The nanotube solution was black and homogeneous while being stirred, but precipitation occurred when stirring was stopped. A 2 mL aliquot of TOP/TOPO-capped InP or CdSe QDs in hexanes (OD of ∼0.5) was added to the suspended SWNTs, and stirring was continued for an additional 18 h at 80 °C under nitrogen. The QR/SWNT assemblies were prepared in chloroform by combining TOP/TOPO-capped CdSe QRs and SWNTs and stirring for 18 h at 40 °C under nitrogen. Specimens mounted on a TEM grid were rinsed twice with either toluene (QD/SWNT) or chloroform (QR/SWNT) to remove excess or weakly bound semiconductor NCs. Four different QD and QR nanoparticles were used in this study (Table 1).

TABLE 1: Size Distributions and Physical Properties of Semiconductor InP and CdSe Colloids

sample	material	shape	diameter (Å)	length (Å)	adsorption ordering on SWNTs
1	InP	dot	43.2 ± 2.1		linear arrays
2	CdSe	dot	33.8 ± 4.0		linear arrays
3	CdSe	dot	23.5 ± 3.3		random
4	CdSe	rod	64.8 ± 3.3	250−330	linear

Figure 1a is a TEM image of 43 Å InP QDs (sample 1) adsorbed on purified SWNTs. The image shows several intertwined SWNT bundles and dark spots that are InP QDs. Although the SWNT surfaces are obscured by a coating comprised of solvent and TOP/TOPO species, lattices fringes can still be observed in QD-free areas, indicating that the SWNTs have not been damaged. Regions where QDs are packed between intersecting SWNT bundles (labeled A) can also be seen as well as short, linear arrays of QDs that lie along the direction of the SWNT substrate (labeled B). Figure 1b shows a different region of the sample where the SWNT bundles are broader and straighter. Here, the TEM image clearly shows a

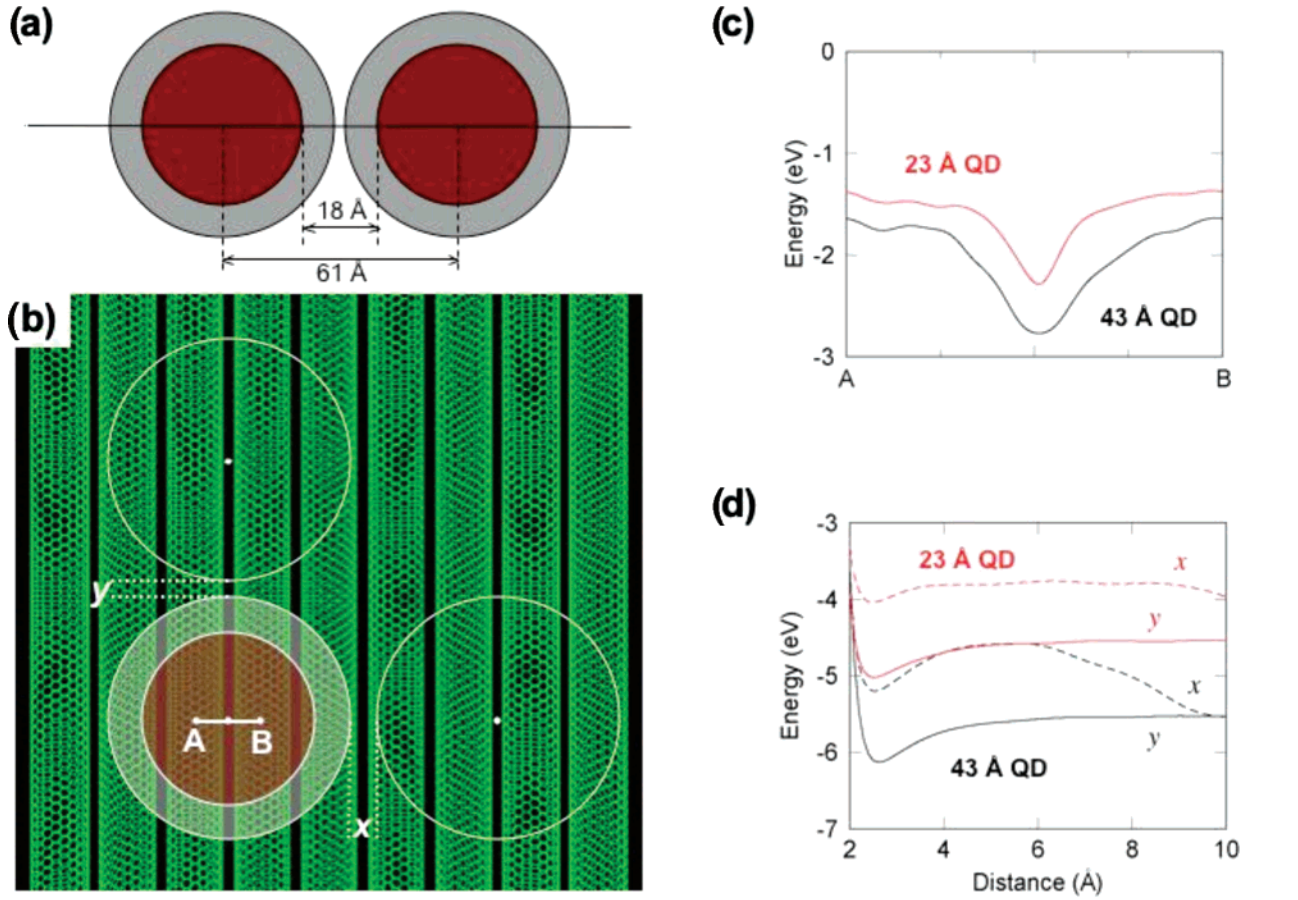

Figure 2. Self-assembly of QDs into linear chains on the SWNT surfaces explained by the inherent QD−SWNT and QD−QD vdW interactions. Minimum-energy configurations for the QDs on a SWNT mat were calculated using a simplified model. (a) The 43 Å InP QDs were modeled as spheres (red) surrounded by a 7.5 Å TOP/TOPO ligand shell (grey). An intervening 3 Å vdW gap separated the two neighboring TOP/TOPO-coated QDs. Therefore, the c−c and e−e separation distances for the two 43 Å InP QDs were 61 and 18 Å, respectively. (b) The substrate on which the QDs were adsorbed was a planar mat of 13.6 Å diameter (10,10) SWNTs separated by a 3.4 Å vdW gap. (c) The variation of the vdW energy for a single QD in contact with the SWNT mat (QD−SWNT) was calculated as function of position as the QD was translated along the A−B line displayed in Figure 2b. (d) The contribution of the QD−QD interactions to the vdW total energy was examined as a function of separation distance for both alignment parallel (*y*, solid curve) and perpendicular (*x*, dashed curve) to the axes of the nanotubes. One QD was kept fixed at a minimum-energy location within a groove between adjacent SWNTs and was considered to be a nucleation point for the addition of the second QD. In Figures 2c and 2d, minimum-energy calculations were determined for both 23 Å (red curve) and 43 Å (black curve) QDs.

tendency for the QDs to align in chains extending along the axes of the SWNT bundles, one of which can be followed for more than 150 nm. The broader, straighter nanotube bundles of Figure 1b apparently favor the formation of the 1-D arrays. Graphical analysis shows an average center-to-center (c−c) separation distance of 61 ± 1 Å for these 1-D QD arrays. Considering that the diameter of the QDs, as determined by absorption spectroscopy and TEM, is 43 ± 2 Å, the average e−e spacing is ∼18 ± 3 Å. Figure 1c shows 34 Å CdSe QDs (sample 2) linearly organized on SWNT surfaces in a similar fashion. In this case, 1-D arrays of more than 20 QDs can be seen extending for more than 100 nm. High-resolution TEM images of the linearly organized 34 Å CdSe QDs (Figure 1c) show a c−c separation distance of 53 ± 1 Å and the same average e−e separation observed for the 43 Å InP QDs (∼18 Å). Isolated QDs were rarely observed for either of these InP and CdSe samples. Washing the assemblies had no significant effect on the TEM images, demonstrating that the QDs were strongly adsorbed onto the SWNTs in the preferred linear arrangements. As a final point, on the basis of the TEM images in Figure 1, there was no evidence for QDs inserting into SWNTs bundles. Theoretical[32] and experimental[33] studies have shown that the vdW binding between SWNTs is quite strong with as much a 2.5 eV per nm of contact area, and therefore, the insertion of QDs into SWNT bundles would be energetically unfavorable.

QD/SWNT assemblies formed using smaller 24 Å CdSe QDs (sample 3) showed lower loading levels and very little organization (Figure 1d). Although small rafts and chains were observed, most QDs were adsorbed as isolated entities. In fact, the small degree of packing and ordering would go unnoticed if the possibility of linear packing had not been observed for the larger QDs. QRs (sample 4) also adsorbed on SWNTs in linear chains, with their long axes parallel to the axes of the nanotubes (Figure 1e). The number of QRs per chain was typically in the range of 3−6, and the chains were similar in length to the QD linear arrays (100−200 nm) observed for the larger QDs in Figures 1a and 1b.

The self-assembly of QDs into linear chains on the SWNT surfaces can be straightforwardly explained by considering the inherent QD−SWNT and QD−QD vdW interactions using a simplified model (Figure 2). QDs were modeled as spheres surrounded by TOP/TOPO ligand shells. The 18 Å QD e−e separation distance observed for the 43 Å InP QDs was modeled as being filled by two 7.5 Å TOP/TOPO layers with an intervening 3 Å vdW gap (Figure 2a). Since the TOP and TOPO

molecules are terminated with CH_3 groups, the surfaces of the ligand shells were treated as exposed hydrogen atoms randomly distributed with a constant surface density on a spherical surface. Thus, each TOP/TOPO encapsulated 43 Å InP QD was modeled as a 58 Å diameter sphere (43 Å core + 2 × 7.5 Å for the two TOP/TOPO shells) having ~1650 surface hydrogen atoms. Atomistic pairwise summation of the Lennard-Jones 12−6 potentials[34] for the H/C (QD−SWNT) and H/H (QD−QD) pairs were performed to determine the minimum-energy configurations for the QDs on the SWNT mat. Parameters for the Lennard-Jones 12−6 potentials were those previously used for describing the vdW interactions between CH_4 and SWNTs.[34] The second-order H/C (QD−QD) and C/C (QD−SWNT) vdW interactions in the model were not included in the calculations. These second-order vdW interactions should follow a similar trend as in the first-order H/H (QD−QD) and H/C (QD−SWNT) vdW interactions. The nanotube substrate was modeled as a planar mat of 13.6 Å diameter (10,10) SWNTs with each SWNT separated by a 3.4 Å vdW gap (Figure 2b). Due to the simplifications made in the model, only the observed trend and variation in the obtained vdW energies are meaningful.

The variation of the vdW energy for a single QD in contact with the SWNT mat (Figure 2c) was calculated as function of position as the QD was translated along the A−B line displayed in Figure 2b. Note that the potential energy surface for the mat is smooth in the direction parallel to the nanotube axes and that only translation perpendicular to the mat needs to be considered for binding of a single QD. The energy of the system was found to be a maximum of −1.7 eV at both points A and B when the 43 Å QD (black curve) was located on top of a SWNT (Figure 2c). When the center of the QD was located within a groove between SWNTs, the QD−SWNT interfacial contact area was maximized, and the vdW energy was a minimum of −2.8 eV (Figure 2c). Thus, it is very likely for the QDs to adsorb at groove sites along the external surfaces of the SWNT bundles.

To probe the contribution of QD−QD interactions to binding and alignment we examined the variation of the vdW total energy for two 43 Å QDs (black curve) on the SWNT mat as a function of separation distance for both alignment parallel (*y*) and perpendicular (*x*) to the axes of the nanotubes (Figure 2d). One QD was kept fixed at a minimum-energy location within a groove between adjacent SWNTs and was considered to be a nucleation point for the addition of the second QD. In the parallel alignment (*y*), both QDs are always situated within a groove so the energy gain for two QDs at large separation distances is simply twice that of an individual QD. When the separation distance is reduced to 2.6 Å, the QD shells interact to produce an additional vdW energy of 0.6 eV. At smaller separations, the energy of the system climbs due to the nuclear repulsion component of the 12−6 potential. Thus, the total energy for the system is minimized at −6.2 eV when the two QDs are in a groove and in vdW contact.

In the perpendicular alignment (*x*) case, the minimum-energy configuration for two 43 Å QDs is higher than the minimum energy obtained for the parallel alignment (*y*) configuration by 0.6 eV (Figure 2d). The minimum-energy configuration in the perpendicular alignment (*x*) case can only be obtained when the two QDs are situated in separate grooves and not interacting. The additional vdW energy of 0.6 eV gained from shell−shell vdW interactions is only obtained when the second QD is located outside of the low-energy groove between SWNTs. A comparison of the parallel and perpendicular alignments clearly shows an energetic preference for QDs to assemble in a closely packed, linear array within a single groove between SWNTs, in agreement with the experimental observations. In this arrangement the sum of the QD−SWNT and QD−QD contact surface areas is maximized to achieve the greatest possible vdW stabilization.

The lack of 1-D ordering for the smallest, 23 Å CdSe QDs can also be qualitatively understood within the vdW model (Figure 2). The vdW energy for the 23 Å QD (red curve) calculated for translation along the A−B line in Figure 2 shows a minimum energy of −1.4 eV (at A or B) and a maximum energy of −2.3 eV when the QD is in a SWNT groove (Figure 2c). The total energy for the two 23 Å QDs (red curve) in the perpendicular alignment (*x*) is never greater than approximately −4 eV for all separation distances, while the parallel alignment (*y*) yields a maximum of approximately −5 eV when both QDs are within the same groove and in vdW contact. In comparison, the maximum energy found for the 43 Å QDs in the parallel alignment (*y*) configuration was 1.1 eV greater than the parallel alignment case for the 23 Å QDs. Thus, the larger QDs have a much larger driving force to self-assemble into 1-D arrays. The energy available to drive ordering of the smaller QDs is apparently insufficient to cause a large degree of ordering and instead produces a more random decoration of the surfaces with the sample preparation methods employed here.

The relatively constant QD e−e spacing of ~18 Å is smaller than that expected for two non-interpenetrating TOP/TOPO shells (2 × 11 Å, or 22 Å)[35] but larger than the 11 Å nearest neighbor distance observed by small-angle X-ray scattering for TOP/TOPO-terminated close-packed QD assemblies.[22,36] The smaller 11 Å interparticle separation distance in the close-packed QD assemblies was explained by compression and/or interdigitation of the ligand molecules in adjacent TOP/TOPO shells. The slightly larger e−e spacing observed with QDs in 1-D arrays on SWNTs would be expected if the TOP/TOPO shells did not interpenetrate to the same degree as in the close-packed QD assemblies. This might be the case if the SWNT substrate played a role in increasing the density of the TOP/TOPO species in the gap between the QDs. In this view, vdW interactions between the tube surfaces and the ligand species could give rise to denser packing and alignment of the TOP/TOPO species along the nanotube axes, which would hinder compression and interpenetration of the QD ligand shells. Regardless of the mechanism, the observation of a constant e−e spacing of ~18 Å demonstrates that the QDs are in fact closely packed in one dimension.

To check for possible derivatization of nanotube surfaces, optical absorption spectra were measured before and after the adsorption of 34 Å CdSe QDs (sample 2). Samples were prepared by spraying solutions onto quartz cover slips, and both samples exhibited the well-known absorption bands associated with the optical transitions between van Hove singularities in the SWNT density of states (Figure 3).[37] If the long lines of closely packed QDs were attached to the SWNT surfaces by derivatization, then a linear arrangement of attachment points would be required, which is highly unlikely. Furthermore, the density of such attachment points would be required to match or greatly exceed the observed c−c QD spacing for the dots to be organized and closely packed. The fact that the SWNT electronic structure is unperturbed after QD attachment indicates that very few, if any, new defects or sp^3-hybridized carbon species were generated by the gentle methods used to prepare the QD/SWNT composites. Consequently, in contrast to other studies,[12−18] SWNT derivatization plays little or no role in producing the 1-D arrays of QDs observed here. We note that the optical absorption associated with the QDs is not observed

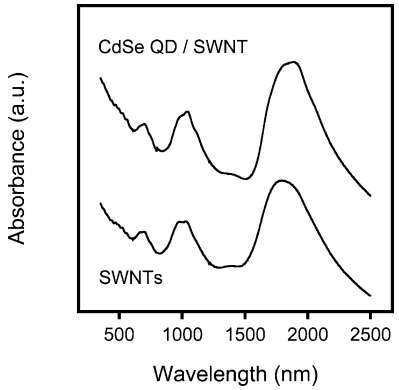

Figure 3. Typical UV−vis−near-IR spectra of CdSe QD (sample 2)/SWNT assemblies (top) and SWNTs (bottom). The samples were prepared by spraying a solution of either SWNTs or the QD/SWNT product onto quartz cover slips.

due to the overwhelming large optical density of the nanotubes at wavelengths shorter than ∼600 nm.

In summary, we have demonstrated a nondestructive method for constructing well-defined, organized NC/SWNT assemblies. The above studies document that the spatial ordering and adsorption of the semiconductor NCs on the SWNT surfaces was dependent on the relative size of the semiconductor NC. Strongly adsorbed, linear assemblies of both QDs and QRs were observed along the surfaces of SWNT bundles. This behavior was driven by the SWNT substrate and interparticle attractions due to vdW energies. Thus, the self-assembly of semiconductor NCs onto SWNT surfaces was accomplished without chemical functionalization of the surfaces of SWNTs with linker molecules. These assemblies may provide a new approach for investigating alternative photocatalytic agents for solar photochemistry.

Acknowledgment. This paper is dedicated to the memory of Olga Mićić. This work was supported by the U. S. Department of Energy Solar Photochemistry Program funded by the Office of Science, Office of Basic Energy Sciences, Division of Chemical Sciences, Geosciences, and Biosciences.

References and Notes

(1) Alivisatos, A. P. *J. Phys. Chem.* **1996**, *100*, 13226−13239.
(2) Avouris, P. *Acc. Chem. Res.* **2002**, *35*, 1026−1034.
(3) *Semiconductor and Metal Nanocrystals: Synthesis and Electronic and Optical Properties*; Klimov, V. I., Ed.; Optical Engineering 87; Marcel Dekker: New York, 2004.
(4) Dresselhaus, M. S.; Dresselhaus, G.; Eklund, P. C. *Science of Fullerenes and Carbon Nanotubes*; Academic Press: San Diego, CA, 1996.
(5) Rao, A. M.; Richter, E.; Bandow, S.; Chase, B.; Eklund, P. C.; Williams, K. A.; Fang, S.; Subbaswamy, K. R.; Menon, M.; Thess, A.; Smalley, R. E.; Dresselhaus, G.; Dresselhaus, M. S. *Science* **1997**, *275*, 187−191.
(6) Ajayan, P. M.; Charlier, J.-C.; Rinzler, A. G. *Proc. Natl. Acad. Sci. U.S.A.* **1999**, *96*, 14199−14200.
(7) Bonard, J. M.; Salvetat, J. P.; Stockli, T.; de Heer, W. A.; Forro, L.; Chatelain, A. *Appl. Phys. Lett.* **1998**, *73*, 918−920.
(8) Dai, H. *Acc. Chem. Res.* **2002**, *35*, 1035−1044.
(9) Kim, Y. H.; Heben, M. J.; Zhang, S. B. *Phys. Rev. Lett.* **2004**, *92*, 176102.
(10) Guldi, D. M.; Rahman, A.; Sgobba, V.; Ehli, C. *Chem. Soc. Rev.* **2006**, *35*, 471−487.
(11) Baughman, R. H.; Zakhidov, A. A.; de Heer, W. A. *Science* **2002**, *297*, 787−792.
(12) Haremza, J. M.; Hahn, M. A.; Krauss, T. D. *Nano Lett.* **2002**, *2*, 1253−1258.
(13) Banerjee, S.; Wong, S. S. *Nano Lett.* **2002**, *2*, 195−200.
(14) Ravindran, S.; Chaudhary, S.; Colburn, B.; Ozkan, M.; Ozkan, C. S. *Nano Lett.* **2003**, *3*, 447−453.
(15) Han, W. Q.; Zettl, A. *Nano Lett.* **2003**, *3*, 681−683.
(16) Li, X. H.; Niu, J. L.; Zhang, J.; Li, H. L.; Liu, Z. F. *J. Phys. Chem. B* **2003**, *107*, 2453−2458.
(17) Banerjee, S.; Wong, S. S. *J. Am. Chem. Soc.* **2003**, *125*, 10342−10350.
(18) Banerjee, S.; Wong, S. S. *Adv. Mater.* **2004**, *16*, 34−337.
(19) Guldi, D. M.; Rahman, G. M. A.; Sgobba, V.; Kotov, N. A.; Bonifazi, D.; Prato, M. *J. Am. Chem. Soc.* **2006**, *128*, 2315−2323.
(20) Collier, C. P.; Vossmeyer, T.; Heath, J. R. *Annu. Rev. Phys. Chem.* **1998**, *49*, 371−404.
(21) Murray, C. B.; Kagan, C. R.; Bawendi, M. G. *Science* **1995**, *270*, 1335−1338.
(22) Murray, R. W.; Kagan, C. R.; Bawendi, M. G. *Annu. Rev. Mater. Sci.* **2000**, *30*, 545−610.
(23) Rogach, A. L.; Talapin, D. V.; Shevchenko, E. V.; Kornowski, A.; Hasse, M.; Weller, H. *Adv. Funct. Mater.* **2002**, *12*, 653−664.
(24) Cho, K. S.; Talapin, D. V.; Gaschler, W.; Murray, C. B. *J. Am. Chem. Soc.* **2005**, *127*, 7140−7147.
(25) Sashchiuk, A.; Amirav, L.; Bashouti, M.; Krueger, M.; Sivan, U.; Lifshitz, E. *Nano Lett.* **2004**, *4*, 159−165.
(26) Dillon, A. C.; Gennett, T.; Jones, K. M.; Alleman, J. L.; Parilla, P. A.; Heben, M. J. *Adv. Mater.* **1999**, *11*, 1354−1358.
(27) Dillon, A. C.; Yudasaka, M.; Dresselhaus, M. S. *J. Nanosci. Nanotechnol.* **2004**, *4*, 691−703.
(28) Micic, O. I.; Jones, K. M.; Cahill, A.; Nozik, A. J. *J. Phys. Chem. B* **1998**, *102*, 9791−9796.
(29) Peng, Z. A.; Peng, X. *J. Am. Chem. Soc.* **2002**, *124*, 3343−3353.
(30) Peng, Z. A.; Peng, X. *J. Am. Chem. Soc.* **2001**, *123*, 183−184.
(31) Peng, X. G.; Wickham, J.; Alivisatos, A. P. *J. Am. Chem. Soc.* **1998**, *120*, 5343−5344.
(32) Girifalco, L. A.; Hodak, M.; Lee, R. S. *Phys. Rev. B* **2000**, *62*, 13104−13110.
(33) Chen, B.; Gao, M.; Zuo, J. M.; Qu, S.; Liu, B.; Huang, Y. *Appl. Phys. Lett.* **2003**, *83*, 3570−3571.
(34) Mao, Z.; Garg, A.; Sinnott, S. B. *Nanotechnology* **1999**, *10*, 273−277.
(35) Micic, O. I.; Ahrenkiel, S. P.; Nozik, A. J. *Appl. Phys. Lett.* **2001**, *78*, 4022−2024.
(36) Jarosz, M. V.; Porter, V. J.; Fisher, B. R.; Kastner, M. A.; Bawendi, M. G. *Phys. Rev. B* **2004**, *70*, 195327.
(37) Kataura, H.; Kumazawa, Y.; Maniwa, Y.; Umezu, I.; Suzuki, S.; Ohtsuka, Y.; Achiba, Y. *Synth. Met.* **1999**, *103*, 2555−2558.